Int. J. Electrochem. Sci., 8 **(2013)** 4761 - 4775

International Journal of
ELECTROCHEMICAL
SCIENCE
www.electrochemsci.org

Electrochemical Behaviour of a Super Austenitic Stainless Steel in Amazonian Aqueous Environment

J. K. Ntienoue, A. Reguer, F. Robert, O. Naït-Rabah and C. Roos[*]

Laboratoire Matériaux et Molécules en Milieu Amazonien, Université des Antilles et de la Guyane, UAG-UMR ECOFOG, Campus Trou Biran, Cayenne 97337, French Guiana.
[*]E-mail: christophe.roos@guyane.univ-ag.fr

Received: 30 November 2012 / *Accepted:* 12 January 2013 / *Published:* 1 Aril 2013

The electrochemical behaviour of 254 SMO super austenitic stainless steel in natural seawater collected from river mouth of French Guiana was investigated. A comparative study of samples immersed during 22 days in this environment was made including influences of scraped biofilm introduced in experiments and of stirring. Electrochemical measurements - open circuit potential (OCP), electrochemical impedance spectroscopy (EIS), cyclic voltammetry (CV) and linear polarisation (LP) - are used to characterize the metal/medium interface included biofilms adhesion. The EDX analysis (EDAX system) shows that the chemical composition of adhered biofilm consists mostly of iron, oxygen, silicon and aluminium and seem preferentially bind on metal defects.

Keywords: Stainless steel, EIS, Cyclic voltammetry, Passive films, ESEM.

1. INTRODUCTION

Many natural and artificial systems are influenced by biofilms, microorganisms firmly attached to surfaces. In this study, a super austenitic stainless steel (SASS) was used because of its chemical composition enriched molybdenum which confers high resistance to corrosion [1,2]. This type of alloy is actually known to develop spontaneously passive nanoscale layer which seems to have semiconductor properties [3]. The presence of the biofilm on the surface of steel can modify chemical constants of the metal/medium interface such as partial pressure of oxygen, pH, and others [4-6]. For example, the presence of enzymes (oxidases) leads to the production of hydrogen peroxide or gluconic acid involving a decrease in pH. And therefore, the presence and growth of biofilm on steel are likely to damage the passive layer and/or involve changes in its electronic properties [7,8].

The climate of the Amazon (tropical) South America is warm and wet most of the year, which promotes the growth of microorganisms. Systematic information on the impact of microorganisms on

materials immersed in seawater or river mouths Amazonian is lacking. It was only in the 80s, some researchers have focused on the observation of the growth of biofilms in this particular environment by scanning electron microscopy [9].

In general, the bacteria are able to oxidize a wide variety of chemical substances; using them as nutriments in order to proliferate [10,11]. The main types of bacteria adhering to the metal are the sulfate-reducing bacteria - SRB, sulfur-oxidizing bacteria - SOB and iron-oxidizing/reducing bacteria – IOB/IRB, manganese-oxidizing bacteria - MOB and bacteria secreting organic acids [12-15].

The majority of studies on behaviour of stainless steel in seawater have been carried out using monocultures of bacteria under well controlled laboratory conditions [16,17]. But in this work, we are interested in studying the behavior of an austenitic stainless steel immersed in water at the mouth of the river Cayenne (Mahury). The objectives are to see if the presence and growth of a biofilm on the metal surface during the first 3 weeks of immersion may alter the electrochemical behavior of the metal / medium interface.

To obtain the necessary information, the technique of electrochemical impedance spectroscopy (EIS) completed by cyclic voltammetry (CV), linear polarization (LP) and environmental scanning electron microscopy (ESEM) coupled to the dispersive spectroscopy of energy (EDS) were used.

2. EXPERIMENTAL

2.1. Materials

A super austenitic stainless steel - SASS - is investigated in this work. The chemical composition is given in table 1.

Table 1. Chemical composition of SASS.

Alloy	%	Ni	Cr	Mo	N	C	Mn	Fe
SASS	Weight percent	17.8	19.9	6.0	0.2	0.01	0.5	Bal.

All the samples are plates of dimensions 80 mm x 20 mm x 1 mm and were provided by the company CEAEA Saclay. The surfaces of SASS were degreased with acetone, cleaned in an ultrasonic bath with distilled water and sterilized with ethanol before exposure. The surface of the sample reveals defects with dimensions ranging from a few micrometers to 200 micrometers (Fig. 1).

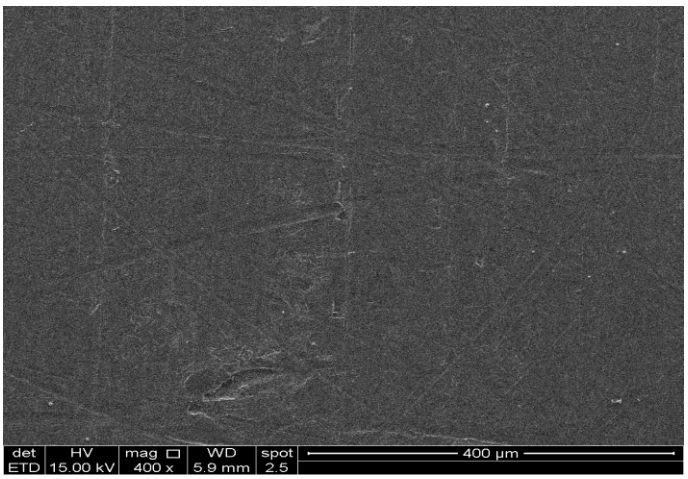

Figure 1. Micrography of the super austenitic stainless steel surface before immersion showing the presence of defects (ESEM).

The electrolyte was chosen on the river mouth Mahury in French Guiana (Estuary to the forefront of the fortress Diamond Remire-Montjoly city). pH and electrical conductivity of natural seawater were measured with WTW inoLab equipment and cation concentrations in stream (Technicon II) using spectrophotometers Methrom or Secoman1000. Chlorine was analyzed by fluorimetry, nitrite by the method based on the Griess reaction applied to seawater by Bendschneider and Robinson. Koroleff method is used for the ammonium and Murphy Riley method for phosphates and silica. Table 2 shows the mean values of the characteristics of electrolytes and concentrations of chemical species in aqueous media. The presence of other components at very low concentrations was noted.

Table 2. Main physico-chemical parameters of river mouth of French Guiana

Parameters	Measured values
Temperature (°C)	22.4
pH	7.6
Conductivity at 25 °C (µS/cm)	33100
Ion concentration	Measured values
Cl (mmole/l)	322.34
NO_3 (µmole/l)	0.63
PO_4 (µmole/l)	0.12
Si (µmole/l)	63.09
NH_4 (µmole/l)	3.33
Ca (mmole/l)	5.86
Mg (mmole/l)	27.98
Na (mmole/l)	213.10
K (mmole/l)	6.01

Some media were sterilized in an autoclave (Tuttnauer 3850 MLV) for 30 minutes at 121 ° C (1.1 bar) and 16.5±0.1 grams of solid biofilms collected on the pontoon were added to non-sterile seawater. Six different experimental conditions (test environments) were selected for the study, and are presented in Table 3.

Table 3. Experimental conditions (Y : Yes; N : No)

Experimental conditions	1	2	3	4	5	6
Sterile	Y	Y	N	N	N	N
Stirring	Y	N	Y	N	Y	N
Scraped biofilm	N	N	Y	Y	N	N

2.2. Electrochemical tests

Electrochemical tests were carried out in a bowl capacity of three liters with three-electrodes system consisting of a saturated calomel electrode (SCE) as reference, Pt electrode as a counter electrode and SASS as working electrode. The Bio-Logic Potentiostat was used in this research work. The open circuit potential (E_{oc}), electrochemical impedance spectroscopy (EIS), cyclic voltammetry (CV) and linear polarization (LP) measurements were undertaken in seawater at room temperature. OCP measurements were carried out continuously. EIS measurements were made at the open circuit potential using a 10 mV amplitude sinusoidal signal over the frequencies ranging from 100 kHz to 10 mHz. CV tests were used to evaluate the biofilms and passive layer responses and were recorded at a scan rate of 1 mV s^{-1}. The studies potential window was from – 0.2 to 1.2 V/SCE. Representations of LP were derived from CV measurements. Each test was performed three times.

2.3. Surface observation/analysis (ESEM/EDS)

Biofilms on the electrodes were imaged using an environmental scanning electron microscope (ESEM – FEI Quanta 250). Samples were observed by electron microscopy directly after monitoring of open-circuit potential. ESEM allows the observation of hydrated samples and does not require any sample preparation. We have used two configurations: one at a chamber pressure of about 60 Pa with a Large Field Detector (LFD) for imaging the electrode surface with a large field of view and with a backscattered electron detector (BSED) used for imaging atomic number contrast. For the second configuration, we used a gaseous secondary electron detector (GSED) at a chamber pressure of about 600 Pa in combination with a Peltier cooled stage for imaging the biofilms in their natural state. The chemical composition of the subjacent substrate was additionally investigated by EDS analysis (Energy Dispersive X-ray spectroscopy; EDAX system).

3. RESULTS AND DISCUSSION

3.1. Open circuit potential

Fig. 2 shows the variations in an open-circuit potential (E_{oc}) versus the exposure time of SASS in several experimental condition including stirring (with or without), sterility (sterile or non sterile) and scraped biofilm (presence or absence) at room temperature (25°C). The OCP increase was not immediate. Indeed there was a lapse of time between the immersion and the beginning of the increase. This "latency time" or "incubation time", is the time needed by the biofilm to adhere and grow on the surface of the samples. Initial values were always between +40 and +280 mV/SCE. In the case of non-sterile seawater the E_{oc} value increases with time until it reaches values ranging between +230 and +350 mV/SCE, comparable with those of the literature [18-21].

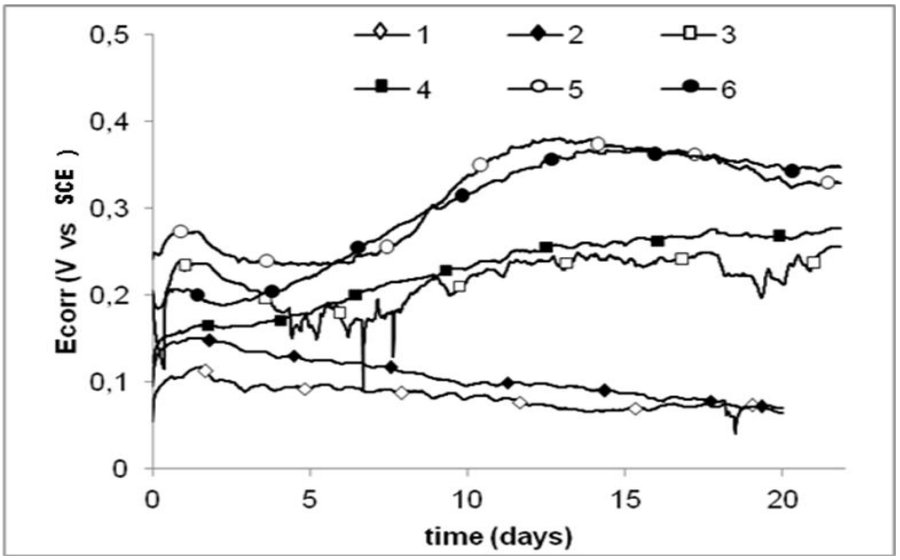

Figure 2. OCP evolution for SASS immersed in the several experimental conditions.

E_{oc} values of the curves obtained in the presence of biofilm scraped on the pontoon were between +315 and +350 mV/SCE and those obtained in the absence of the latter were between +230 and +280 mV/SCE. One can notice that for the non-sterile seawater, the OCP values are close at the end of the experiment (22 days) suggesting that the presence of a scraped biofilm and the stirring did not influence the long-term experiments. OCP values are relatively close for short periods (less than 5 days) 2 by 2 depending on agitation. But after 5 days, when the incubation time is exceeded, the stirring does not seem to have an influence on biofilm development. In contrast the E_{oc} in the sterile seawater decreased initially with the first five days, and after relatively stabilized until it reached values between + 64 and + 69 mV/SCE throughout the 22 days of exposure. The ennoblement of samples is generally interpreted as reflecting the presence of biofilm on the metal surface [22]. Small perturbations on OCV curves resulting, first, by a slight decrease (millivotls few) and then by small

increases in the potential are probably induced by breaks in the passive layer followed by a repassivation of the metal (Fig. 2) [7,23].

3.2. Electrochemical impedance spectroscopy

Fig 3a shows the typical Nyquist plots obtained for SASS in the six experimental conditions. All curves are very close to each other; they do not give real information. Fig.3.b shows the equivalent circuit proposed to simulate the experimental impedance diagram in the evaluation of SASS for experiments where R_S and R_P represent respectively the electrolyte and sample surface (including passive layer) resistances. The equivalent circuit is completed by a constant phase element (CPE) because of the microscopic roughness of the surface and non-ideal capacitive response of the interface stainless steel/solution. The impedance of CPE is written as:

$$Z_{CPE} = Y_0^{-1} (j.\omega)^{- ap}$$

where ω is the angular frequency in rad/s, Y_0 denotes the admittance magnitude of CPE which can be converted into capacitance, while the value of a_p is associated with the non-uniform distribution of current as a result of roughness surface [24].

a)

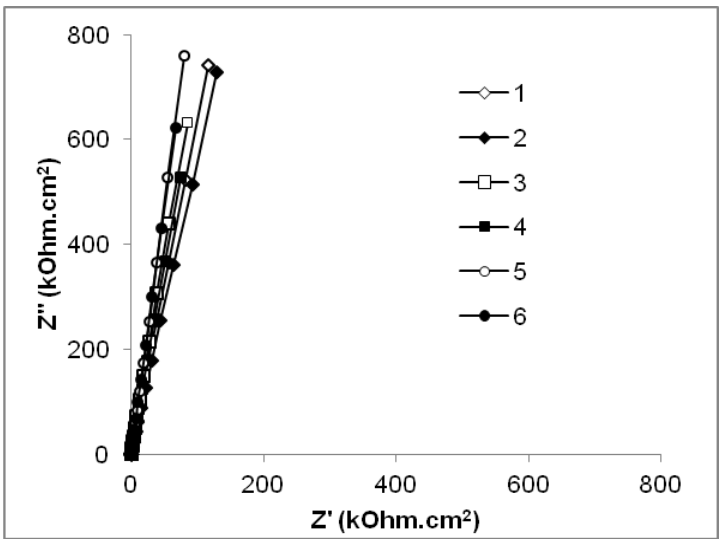

b)

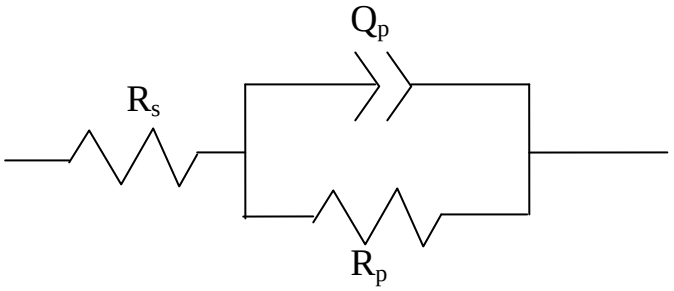

Figure 3. a) Nyquist plots obtained for SASS in the 1-2-3-4-5-6 conditions after 22 days of experiment, b) equivalent circuit used for the modelling of impedance spectra.

Table 4. Results of the fit with the equivalent circuit for Fig. 2b for SASS in experimental conditions 2, 4 and 6 (without stirring).

Experimental conditions	R_p ($\Omega.cm^2$)	Y_0 ($\mu F.cm^{-2}$)	a_p
2	3.96E6	1435	0.89
4	1.21E6	831	0.92
6	5.62E6	739	0.93

It is often very difficult to match the model to experimental data. Indeed, the acquisition of points at low frequencies is sensitive to potential variations including the phenomena of depassivation / repassivation of steel but also probable changes of semiconducting properties of the passive layer due to the presence of biofilm on the surface.

The values of the electric parameters obtained by simulating experimental impedance diagrams for different impedance diagrams using the equivalent circuit are shown in Table 4 (only experiment without stirring). Data values for each parameter were less than 20% error. The presence of biofilm does not affect the impedance of the system because of the values of same order of magnitude obtained for R_p. The capacitance value decreases slightly in presence of biofilm while a_p values increase, that could be explained the tendency of biofilm to fix himself in the heterogeneities of the surface.

Bode plots (Fig. 4) show that, at high frequencies, the impedance of the system is higher in non-sterile condition. High frequencies highlight the fast phenomena such as charge transfers which occur at metal/solution interface including passive film. An increase of impedance in presence of biofilm indicates a decrease of charge transfers. It is possible that this difference is related to a modification of semi-conductivity properties of the passive layer.

a)

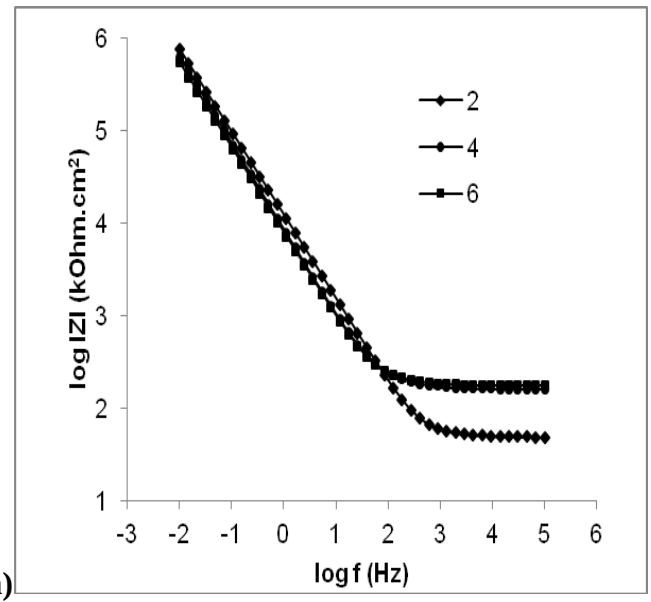

b)

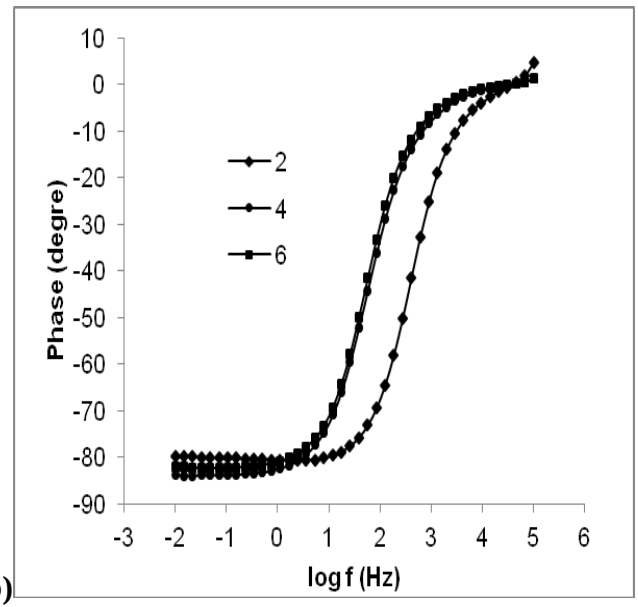

Figure 4. Bode plots obtained for SASS in the 2-4-6 conditions after 22 days of experiment; (a) Modulus versus frequency; (b) phase angle versus frequency.

3.3. Cyclic voltammetry

Cyclic Voltammetry was used to understand biofilm activity on the electrodes surface. The Fig. 5 shows the first cycle of experiments without stirring (2, 4 and 6). Above 1V versus SCE is observed for the three curves the oxidation peak of H_2O. It is also observed for the 3 curves a small oxidation peak around 0.6 V vs. SCE and the reduction peak corresponding to - 0.2V versus SCE. These peaks probably correspond to the signature of the passive layer formed on SASS. In non-sterile conditions, two other peaks are present in oxidation to 0.8V and 0.95V versus SCE; they are no longer visible under reducing conditions. These peaks are probably related respectively to the oxidation of Fe (II) to Fe (III) and Cr (III) to Cr (VI) [25]. Nevertheless, the fact that the associated reductions do not appear suggest that these new species formed during oxidation scanning probably disappeared. If the iron element can come from both the metal and the medium (but probably not from the medium as shown by the EDX analysis presented in section 3.4), it is not the case of chromium which is totally absent from the medium. It confirms that the presence of the biofilm at the interface metal/medium introduces modifications of the chemical composition of the passive layer.

Figs. 6a and 6b expose four successive cycles respectively for the samples in conditions 4 and 6. These curves confirm the disappearance of peaks at 0.8 and 0.95V oxidation compared with SCE since they no longer appear in cycles 2, 3 and 4 for which the curves are superimposed.

The cyclic voltammetry study shows, however, that the presence of biofilm alters the chemistry of the interface. It is possible that the presence of species that oxidize (Cr^{3+} and Fe^{2+}) reflects a chemical modification of the passivation layer due to a change in the diffusion regime.

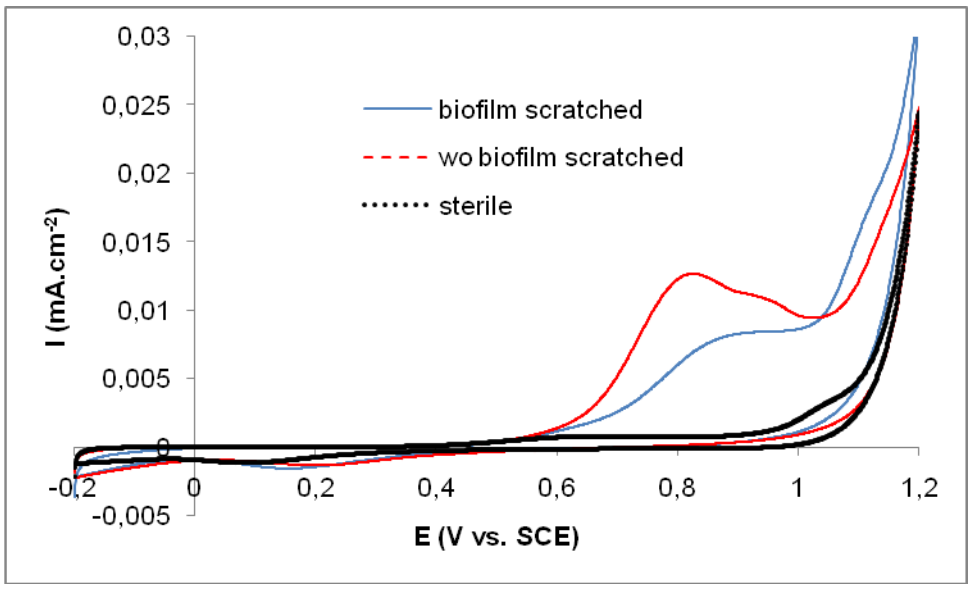

Figure 5. Cyclic voltammograms : first cycle of each experimental condition without stirring of SASS after 22 days of experiment.

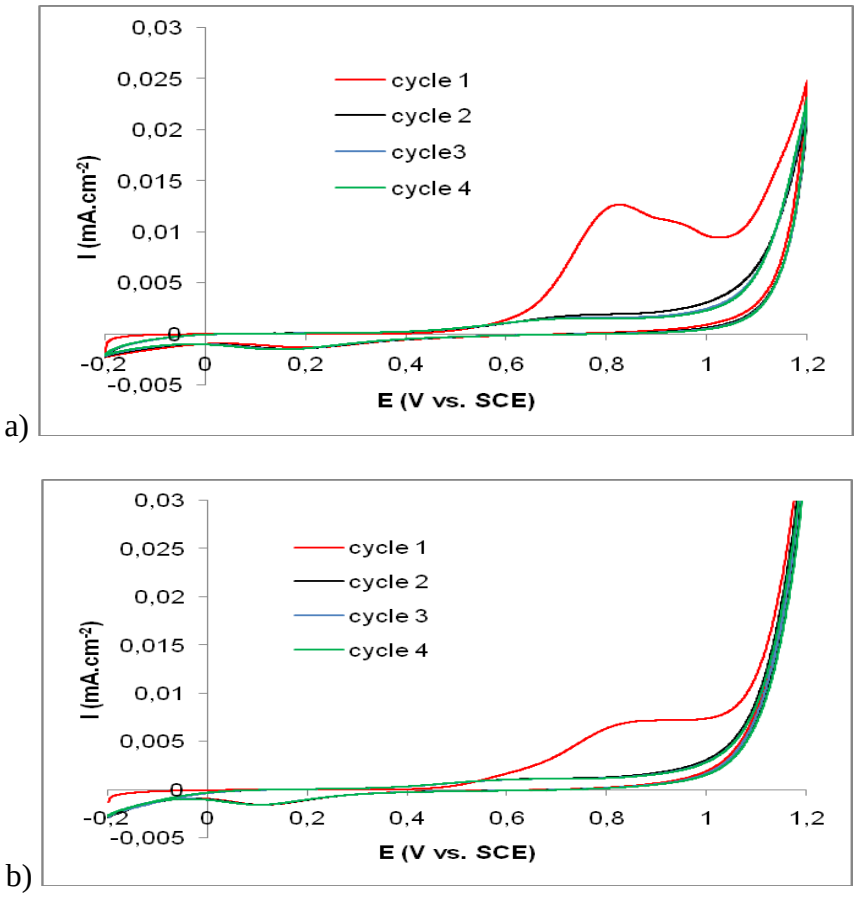

Figure 6. Cyclic voltammograms of SASS after 22 days of experiment: 4 successives cycles for experimental conditions without stirring; (a) with biofilm scratched (condition 4); (b) without biofilm scratched (condition 6).

Fig. 7 shows the anodic part of the linear polarization curve for sterile and non-sterile experiments performed without stirring. It may be noted that there is a passivation region on the 3 curves. However, it begins to overvoltage smaller (about +0.5 V) to the sample in a sterile environment and takes longer to +0.9 V. For non-sterile environments, passivation plateau is between +0.8 and about 1.05V and is shifted to higher currents. This also confirms that the passive layer is affected by the presence of biofilm. The increase of the passivation current by a factor 10 in the presence of biofilm indicates that the electronic exchanges are increased for a given voltage. This is in the sense that the semiconducting properties of the passive layer would change.

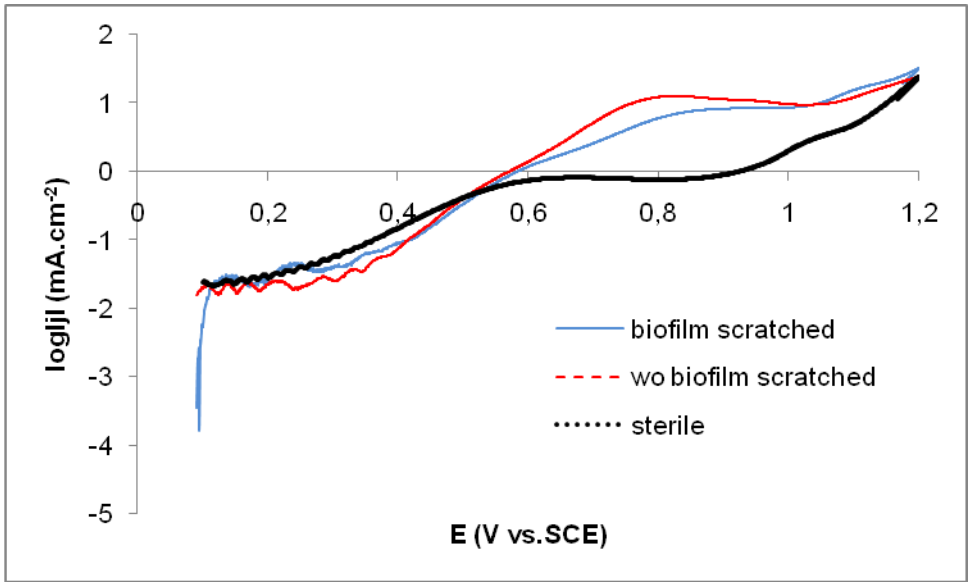

Figure 7. Anodic curves of SASS after 22 days of experiment for each experimental condition without stirring.

3.4. Surface observation/analysis (ESEM/EDS)

ESEM/EDS system was used i) to observe the evolution of the colonization of the biofilm on the SASS surface during the first 30 days of immersion, ii) to confirm the presence of bacteria and exopolymers on his surface and iii) to quantify the chemical compositions of the biofilm adhered.

The images in Fig. 8 performed with a BSE detector shows the evolution of the colonization of the biofilm on the surface of the SASS as a function of immersion time (up to 30 days) and express the associated coverage ratio. The elements entering in the composition of the biofilm, having atomic numbers lighter than the elements of the SASS used as electrode, appeared in dark grey or black on the picture. The calculation of coverage ratio was made with image processing software dividing the white zone area by the zone area. The coverage ratio increases with the immersion time but tends to a limit of about 42% after 30 days immersion.

a)

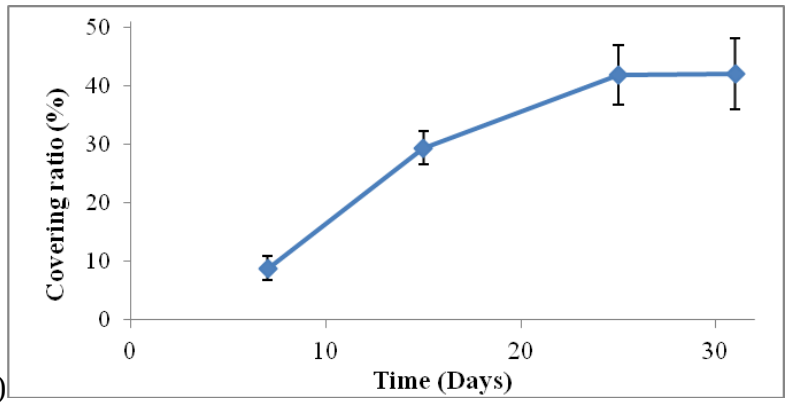

b)

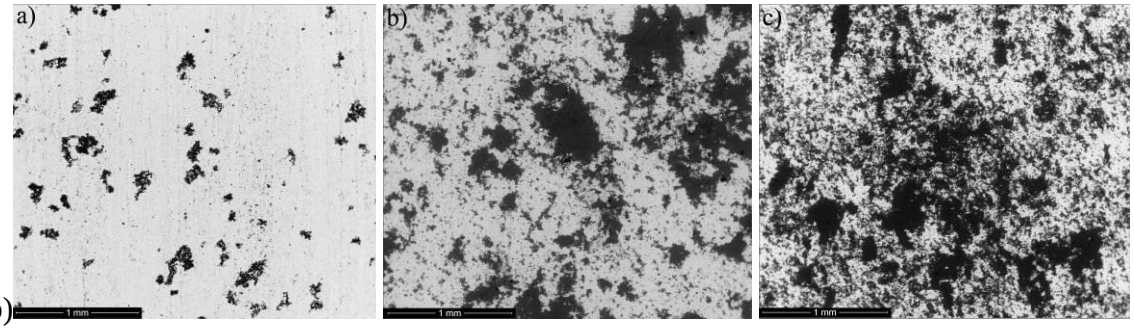

Figure 8. a) Evolution of covering ratio versus time; b) BSE images of 254 SMO SS Surfaces versus time exposition 7 days, 15 days and 30 days in condition 4.

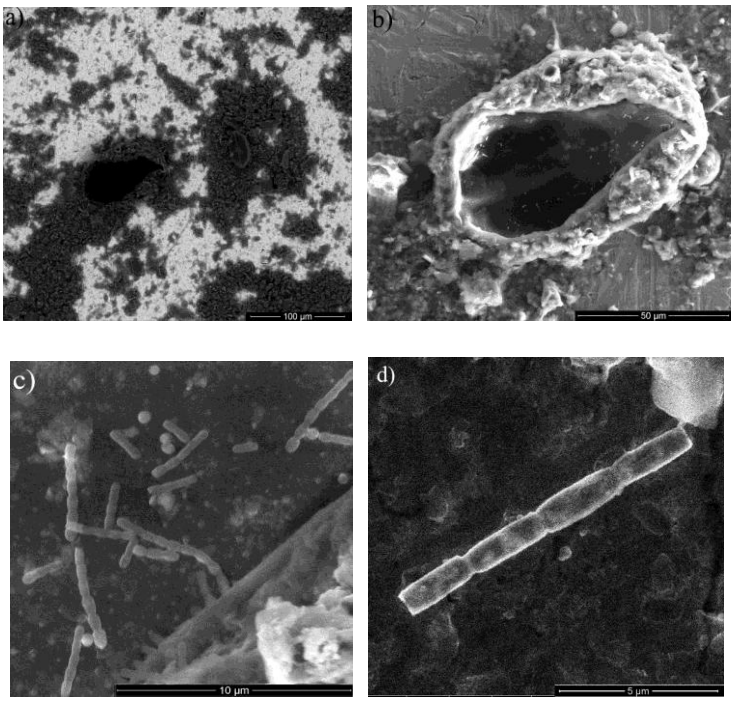

Figure 9. Micrographies of the biofilm on SASS in condition 4 after 22 days of experiment a) Detector BSED, x 400, Pressure 60 Pa, acceleration voltage 15 Kev b) Detector LFD, x 1 200, Pressure 60 Pa, acceleration voltage 15 Kev c) Detector LFD, x 16 000, Pressure 60 Pa, acceleration voltage 10 Kev d) Detector GSED, x 24 000, Pressure 600 Pa, acceleration voltage 10 Kev

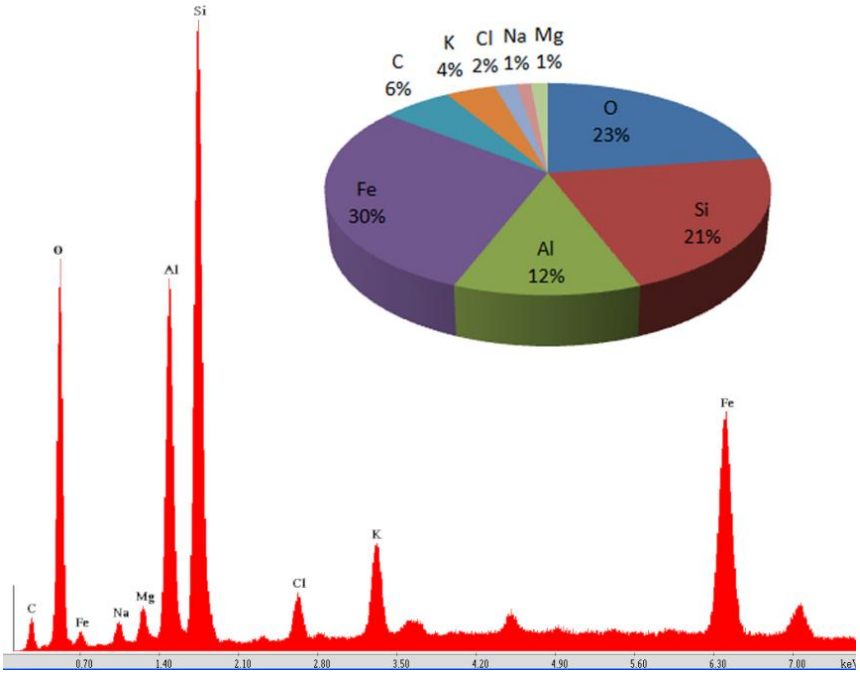

Figure 10. EDX analysis of biofilm in condition 4 with Detector BSED, x 4000, Pressure 1.10^{-4} Pa, acceleration voltage 20 Kev

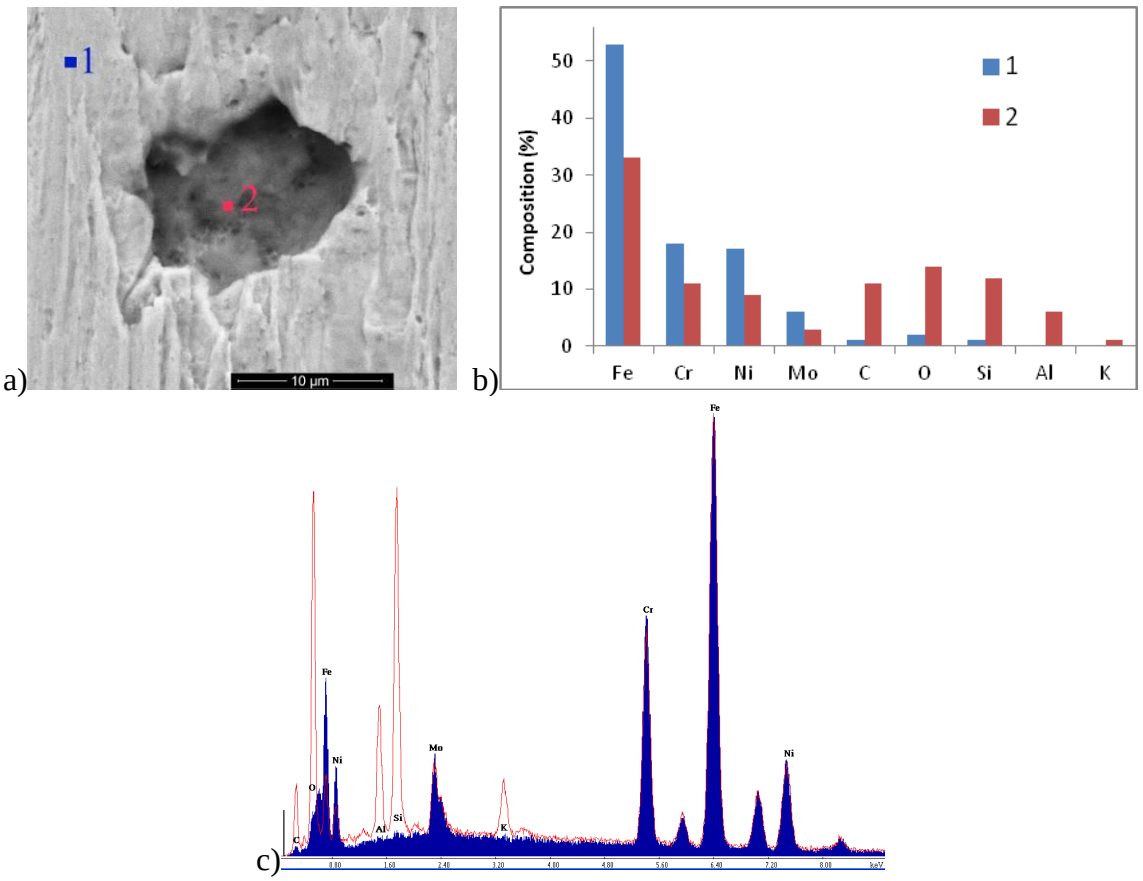

Figure 11. EDX analysis of a defect with Detector BSED in condition 4 with, x 4000, Pressure 1.10^{-4} Pa, acceleration voltage 20 Kev for SASS after 22 days of experiment, a) EDS micrography (points 1 and 2), b) corresponding quantitative results, c) corresponding spectra.

The micrographies in Figs. 9a, b, c and d show the morphology of the biofilm at different magnifications using several detectors. These show the presence of a complex biofilm including aggregates regularly distributed over the surface and lined with exopolymers. They clearly reveal that many bacteria are present. Some authors have also put them in evidence [26-28]. The chemical composition of biofilm on the material surface (made by EDS) is given in Fig. 10. The biofilms are majority composed of aluminosilicate (Al-Si-O), Fe and C with trace of salts minerals (Na, Cl, K, Mg).

After cleaning the sample by a slight ultrasonic pickling, a chemical composition map by means of EDS analysis on the surface of the sample covering the defect (Fig. 10) reveals the presence of aluminosilicate elements (Al-Si-O) and depletions of metallic elements (Fe-Cr-Ni-Mo).

Fig. 11a is a picture performed with a BSE detector of steel surface under experimental conditions. Two EDS analyzes to point 1 (outside the defect) and point 2 (bottom defect) are given in Figs. 11b and c. The analysis of point 1 corresponds to the composition of the SASS. The analysis of point 2 gives a chemical composition which incorporates the elements present in the alloy and in the biofilm. The biofilms seem preferentially bind on metal defects.

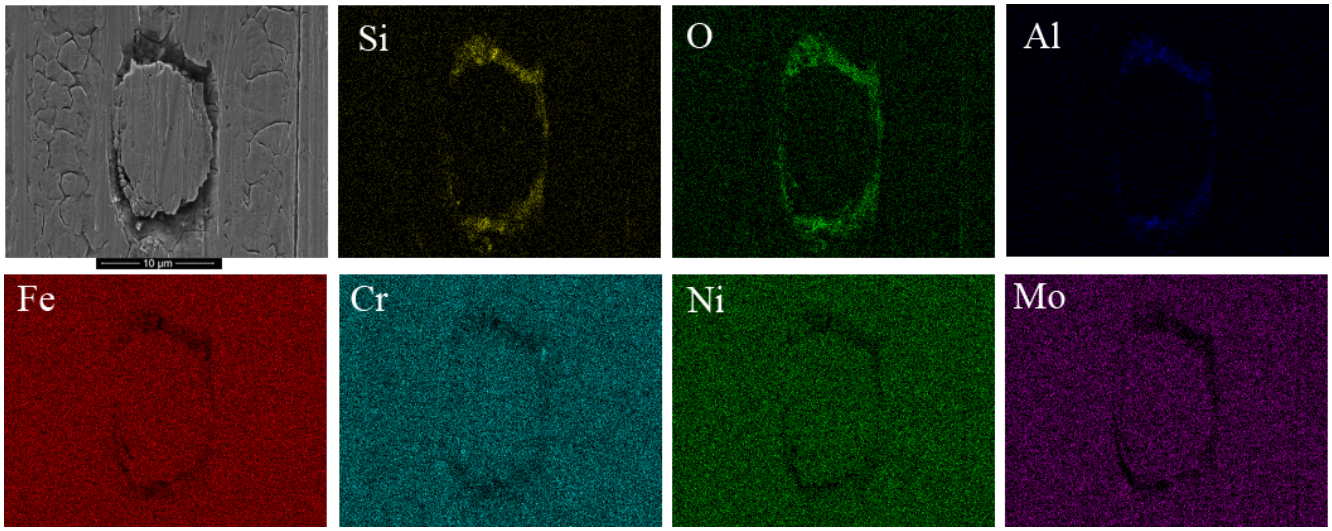

Figure 12. EDX chemical mapping of defect for SASS after 22 days of experiment (condition 4).

Figure 12 which is a X Ray mapping of the surface incorporating a defect of microstructure confirms that biofilm probably settled here preferentially with compounds such aluminosilicates corresponding to depletions of metallic elements (Fe-Cr-Ni-Mo).

4. CONCLUSION

This study provided the behaviour of SASS immersed in Amazonian aqueous environment during the 22 first days. The use of electrochemical techniques showed that in non-sterile conditions :

i) the open circuit potential is shifted to higher potentials compared to sterile conditions. It seems that scraped biofilm and stirring do not influence the long-term experiments.

ii) at high frequencies, the impedance is higher in presence of biofilm.

iii) the presence of peaks oxidation probably related to the oxidation of Fe^{2+} and Cr^{3+}, the latter certainly from the material.

iv) the passivation plateau was shifted to higher currents and existed for a potential range smaller compared to sterile conditions.

The use of ESEM highlighted :

i) the presence of bacteria on the surface.

ii) a rate of coverage of the surface of about 42% by biofilm.

iii) the presence of compounds such aluminosilicates in the surface defects.

In conclusion, electrochemical measurements and EDX analysis indicate that the presence of biofilm on solide surface plays an important role in the behaviour of the SASS in amazonian aqueous environment (biofilm seems to impact the passive layer properties).

ACKNOWLEDGEMENTS

The authors wish to thank IRD (French Guiana Office) for physicochemical analysis, CEAEA for SASS samples and Europe through the Po-feder No. 30931 "Metalsurf".

References

1. R. Qvarfort, *Corr. Sci.*, 40 (1998) 215-223.
2. F. Dabosi, G. Beranger, B. Baroux, *Corrosion localisée*, Les éditions de physique, (1994).
3. J. W. Schultze, M. M. Lohrengel, *Electrochim. Acta*, 45 (2000) 2499-2513.
4. K. Krishnathasan, *pragmatic effects of flow on corrosion prediction*, NACE International, (2009).
5. E. Ilhan-Sungur, N. Cansever, A. Cotuk, *Corr. Sci.*, 49 (2007) 1097-1109.
6. Z. Lewandowski, W. Dickinson, W. Lee, *Water Science and Technology*, 36 (1997) 295-302.
7. V. L'Hostis, C. Dagbert, D. Feron, *Electrochim. Acta*, 48 (2003) 1451-1458.
8. C. Marconnet, Y. Wouters, F. Miserque, C. Dagbert, J.-P. Petit, A. Galerie, D. Féron, *Electrochim. Acta*, 54 (2008) 123–132.
9. S.R. Richards, R.J. Turner, *Water Res.*, 18 (1984) 767-773.
10. I.G. Chamritski, GR. Bums, B.J. Webster, *Corrosion*, 60 (2004) 658-669.
11. L.H. Lin, G.E. Michael, G. Kovachev, H. Zhu, R.P. Philp, C.A. Lewis, *Organic Geochemical*, 14 (1989) 511-523.
12. P. Linhardt, *Biodegradation*, 8 (1997) 201-210.
13. P. Linhardt, *Electrochim. Acta*, 51 (2006) 6081-6084.
14. 24. E. Skavås, A. Adriaens, T. Hemmingsen, *Int. J. Electrochem. Sci.*, 1 (2006) 414-424.
15. V. K. Gupta, B. Sethi, N. Upadhyay, S. Kumar, R. Singh, L. P. Singh, *Int. J. Electrochem. Sci.*, 6 (2011) 650 – 663.
16. El-S. M. Sherif, E. A. El-Danaf, M. S. Soliman, A. A. Almajid, *Int. J. Electrochem. Sci.*, 7 (2012) 2846 – 2859.
17. El-S. M. Sherif, A. A. Almajid, A. K. Bairamov, E. Al-Zahrani, *Int. J. Electrochem. Sci.*, 6 (2011) 5430 – 5444.
18. K. R. Braughton, R. L. Lafond, Z. Lewandowski, *Biofouling*, 17 (2001) 241-251.
19. G. Berthomé, B. Malki, B. Baroux, *Corr. Sci.*, 48 (2006) 2432-244.

20. T.K. Anaka, S. Tsujikawa, *Corrosion Engineering*, 52 (2003) 495-507.
21. A. Iversen, *British Corrosion Journal*, 36 (2001) 277-283.
22. H.A. Videla, *International Biodeterioration and Biodegradation*, 48 (2001) 176-201.
23. V. L'Hostis, C. Dagbert, D. Feron, *Electrochim. Acta*, 48 (2003) 1451-1458.
24. M. Faustin, M. Lebrini, F. Robert, C. Roos, *Int. J. Electrochem. Sci.*, 6 (2011) 4095-4113.
25. M. E. G Lyons, M. P. Brandon *Int. J. Electrochem. Sci.*, 3 (2008) 1463-1503.
26. J. Xu., C. Sun, M. Yan, F. Wang, *Int. J. Electrochem. Sci*., 7 (2012) 11281-11296.
27. C. Marconnet, C. Dagbert, M. Roy, D. Féron, *Corrosion science*, 50 (2008) 2342-2352.
28. F.M. AlAbbas, R. Bhola, J.R. Spear, D.L. Olson, and B. Mishra, *Int. J. Electrochem. Sci.*, 8 (2013) 859-871.